Exploration and Improvement of Room Temperature Properties for Organosilicon Slag Riser

Jljun Lu [a] [iD], Zhuofan Zhong [a] [iD], Yongluan Hu [b] [iD], Di Wu [a] [iD], Huafang Wang [a, *] [iD]

[a] School of Mechanical Engineering and Automation, Wuhan Textile University, China
[b] Wuhan Hanyuan Technology Development Co., Ltd, China
* Corresponding author: E-mail address: wanghfhust@163.com

Abstract

Organosilicon slag, generated as a waste product from organosilicon monomer production, had limited options for resource utilization. Previous experiments utilized recovered organosilicon slag to partially replace heating materials in preparing exothermic insulating risers. However, the incorporation of organosilicon slag led to specific issues in the risers including low compressive strength, high resin addition requirement and easy ignition during drying. In order to address these problems, this study analyzed the effects of resol resin parameters and organosilicon slag on the ambient temperature properties of heating insulating risers through single-factor experiments. In addition, adjustment was made to the drying process and an optimal preparation scheme was determined via orthogonal experiments. The purpose of the study was to prepare risers with reduced resin content, increased organosilicon slag addition and adequate compressive strength. Results showed that selecting a resin viscosity of about 170 mPa.s and resin addition of about 13% allowed for relatively good compressive strength and air permeability with less resin required. Additionally, an organosilicon slag addition of 18-21% and particle size under 30 mesh(550 μ m) was beneficial for improving compressive strength. Adjusting the drying process to a two-step heat preservation approach (180°C for 25 min, then 130°C for 35 min) slightly decreased compressive strength compared to the original process; nevertheless, it improved air permeability and prevented the risers from igniting spontaneously during subsequent drying. The optimized preparation scheme determined through orthogonal experiments involved 150 mPa.s resin viscosity, 14% resin addition, 21% organosilicon slag addition and slag particle size less than 30 mesh (550 μm). This yielded a compressive strength of 4.21MPa and air permeability of 75.6, exceeding the standard of the exothermic insulating riser: GB/T13040-2017.

Keywords: Organosilicon Slag, Resol resin, Drying Process, Compressive Strength, Air Permeability

1. Introduction

Exothermic insulating risers were typically composed of heating materials, insulating materials, refractory aggregates, oxidants, and fluxing agents. The interaction between these various materials achieved suitable heating temperature and insulation time, ultimately improving the shrinkage compensation efficiency during casting. Moreover, the preparation process necessitated the incorporation of an adequate binder amount to ensure sufficient compressive strength and air permeability of the riser. Previous studies had examined different aspects of performance. The effect of material composition and proportions on heating and insulation properties was studied [1], and the heat exchange coefficient between the riser surface and surroundings was evaluated [2]. Shrinkage defects could be influenced by different riser types in

ductile iron castings [3]. Modeling and simulation was used to improve riser efficacy for reducing defects [4]. However, relatively less attention has been paid to conventional properties like compressive strength. Indeed, these performance indices are equally crucial for risers. Adequate strength could minimize loss from impact during transportation and withstand the hydrostatic pressure of molten iron during casting. Appropriate air permeability could enable smooth discharge of gases during casting, avoiding sand-sticking defects on the casting surface.

Organosilicon slag was produced in large quantities as a byproduct during the synthesis of organosilicon monomers (especially methyl chlorosilane monomers). After separation, it was typically disposed of by incineration or landfilling, with limited options for resource utilization. However, the toxicity of the organosilicon slurry could be reduced through hydrolysis, and the added value of the organosilicon slag could be retained from the steam rinsing process, enabling resource utilization [5]. Previous experiments utilized the treated organosilicon slag to produce exothermic insulating risers, meeting the standards for conventional risers in terms of heating performance and insulation time while reducing production costs[1]. However, risers incorporating organosilicon slag displayed issues including low strength, high resin addition requirements, and easy ignition during drying. Simply increasing the resin amount would lead to new problems, like potentially causing high gas emissions [6].

This study focused on preparing exothermic insulating risers utilizing less resol resin and more organosilicon slag while maintaining compressive strength as much as possible. The test sequence initially involved the examination of the effect of resin viscosity on compressive strength at a fixed slag addition to determine the optimal viscosity range, followed by investigating the influence of resin addition on the compressive strength and air permeability to ascertain the suitable addition range. After optimization of the resin viscosity and addition, the effects of organosilicon slag addition and particle size on compressive strength and air permeability were studied respectively. Finally, after completing the above research, the drying process of the exothermic insulating riser was adjusted. Orthogonal experiments were then used to optimize the preparation scheme of the riser.

2. Materials and instruments

2.1. Materials

The raw materials for the riser included organosilicon slag derived from organosilicon slurry produced by Yichang Xingrui Co., Ltd. Table 1 shows the composition of the organosilicon slag. The aluminum powder with a 30-80 mesh particle size was supplied by Zouping Weijia New Materials Co., Ltd. The additives were furnace ash, manganese dioxide, potassium nitrate, and cryolite powder, with the four powder reagents being analytically pure. Hollow floating beads with a particle size of 30-100 mesh are produced by Xingtai Shuyong Refractory Materials Co., Ltd.

Table 1.
Chemical analysis of organosilicon slag

Element	Si	Fe_2O_3	$CuCl_2$	C	Water	Others
	50%	2.99%	0.85%	25%	15.9%	5.26%

The binder for risers is PF-4332 thermosetting resol resin with viscosity ≤1760mPa.s, free phenol ≤10.90%, free formaldehyde ≤0.5%, moisture ≤3.85%, pH=7.03, solid content was 74.13%, residual carbon ≤47.85%. The diluent solvent exploits industrial ethanol with a purity of ≥95%.

2.2. Sample preparation

Cylindrical molds with dimensions of Φ50×50mm were used to prepare the samples. Firstly, raw materials were weighed to a specific proportion and mixed in a sand mixer for 5 min at 140 rpm. Next, the ethanol-diluted resin solution was stirred for 9 min at 285 rpm. After mixing, a certain amount of the mixture was placed into the molds and compacted into specimens using a hammer impact molding machine with five strikes. The prepared specimens were sent to an electric blast drying oven for drying and curing to constant weight, then removed and tested for properties, including compressive strength and air permeability.

2.3. Testing instruments and methods

SWY hydraulic universal testing machine was used to test the compressive strength of specimens; STD-III automatic electric permeability tester was utilized to measure the air permeability of specimens; HWP22-10S solid flash point tester was exercised to determine the flash point of organosilicon slag; SNB-2 rotary viscometer was employed to measure the viscosity of resol resin; Electric blast drying oven was exploited for heat treatment; Field emission scanning electron microscope was used to observe the microstructure morphology of specimens; LS-609 laser particle size analyzer was harnessed to analyze the particle size distribution of organosilicon slag [1].

3. Experiment methods

The properties of organosilicon slag: The micromorphology, particle size distribution, and self-ignition point of organosilicon slag were analyzed.

Single-factor experiments on resol resin: Firstly, the effect of resin viscosity on compressive strength was investigated under the 12% resin addition. After the suitable resin viscosity was determined, the effects of resin additions on compressive strength and air permeability of risers were studied. The selection of resin viscosity and addition ranges referred to the binder parameter used in the existing research of exothermic insulating risers [7]. Besides, the range of resin addition would be at most 15% due to the high resin cost.

Single-factor experiments on organosilicon slag: After select suitable resin parameters, the effects of different additions and

particle sizes of organosilicon slag on the compressive strength and air permeability of risers were analyzed respectively. The experimental ranges for the organosilicon slag factors were selected based on preliminary experimental studies and slag properties. Variable ranges of single-factor experiments were shown in Table 2.

Effects of the drying process on room temperature properties: Two drying processes were analyzed by comparing drying rates, compressive strength and air permeability of risers.

Table 2.
Variable ranges of single-factor experiments

Factor	Variable ranges						
Resin viscosity (mPa.s)	90	130	170	210	250	290	330
Resin addition (%)	11	12	13	14	15	-	-
Organosilicon slag addition (%)	18	21	24	27	-	-	-
Organosilicon slag practice size(mesh)	>30	>40	>50	>60	-	-	-

Orthogonal experiment: an L9(3^4) orthogonal experiment optimized the preparation scheme by adjusting resin viscosity, resin addition, organosilicon slag addition and particle size, based on the adjusted drying process. Variable level of the orthogonal experiment was shown in Table 3.

Table 3.
Variable level of the orthogonal experiment

	Factor			
Level	A Resin viscosity (mPa.s)	B Resin addition (%)	C Organosilicon slag addition (%)	D Organosilicon slag practice size(mesh)
1	190	12	18	>30
2	170	13	19.5	>40
3	150	14	21	>50

4. Results and discussion

4.1. The properties of organosilicon slag

As the organosilicon slag originated from silicone slurry, serious environmental pollution could be caused by the copper chloride or organochlorosilane present if used directly without treatment. Therefore, the method combined hydrolysis and steam rinsing was used to treat it harmlessly, thereby removing the strong acids, metal salts, and organic compounds originally contained in the organosilicon slag [5]. As shown in Fig. 1, characteristic peaks of Si and CuCl were contained in the spectrum of organosilicon slag before harmless treatment, while only the characteristic peaks of Si remained detectable after treatment, with almost no peaks

from other substances observable. Compared to conventional exothermic agent like aluminum powder, though the small residual amout of organic compounds might led to slightly higher gas emissions during combustion, this situation could be mitigated in a ventilated environment. Overall, the treated organosilicon slag could be beneficially utilized as a recycled resource.
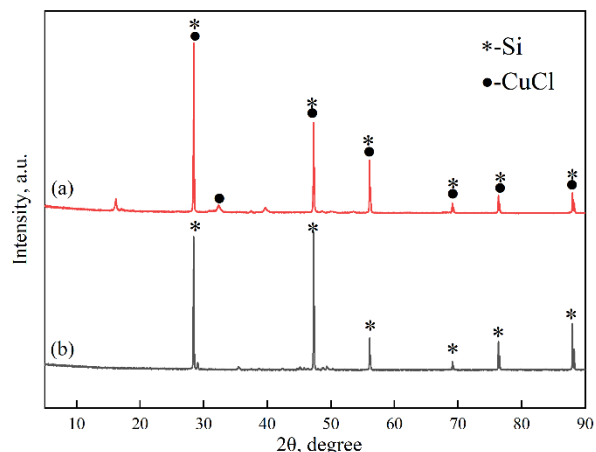

Fig. 1. XRD spectrum of organosilicon slag
（a - organosilicon slag before treatment, b - organosilicon slag after treatment）

The micromorphology of the organosilicon slag was depicted in Fig. 2. Organosilicon slag was obtained through the hydrolysis and steam rinsing of organosilicon slurry, bore similarity to the mud precipitates resulting from flocculated composite fertilizer mixtures [8]. A majority of the particles were characterized by irregular, lump-like floccules possessing loose, porous surfaces and hollow internal structures. The small overall inter-particle distances evidenced an obvious agglomeration of the organosilicon slag particles. Numerous fragmented particles were found to be attached to the large particles. While this structure conferred superior air permeability, the particle strength was lower [9]. Distinct sections and edges, likely resulting from the disaggregation of large particles subsequent to mechanical crushing, were visible in the particles at the intermediate scale.
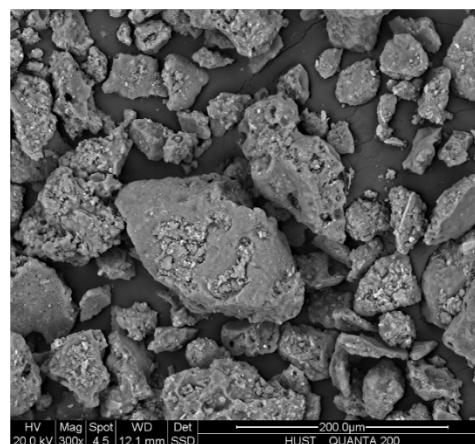

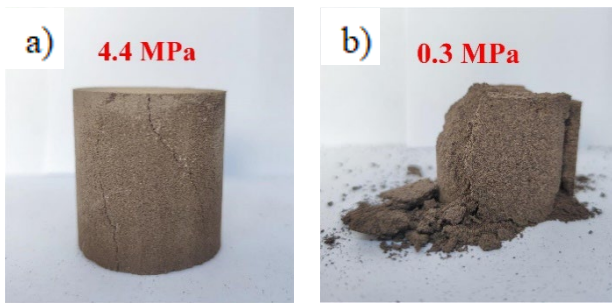Fig. 2. The micromorphology of the organosilicon slag

Fig. 3. Different riser samples under pressure test: 5% organosilicon slag (a), 25% organosilicon slag (b)

As shown in Fig. 3, exothermic insulating risers with more added organosilicon slag were increasingly prone to fracturing under pressure testing. The riser with the highest slag content showed severe surface powdering and direct collapse during testing, indicating extremely low compressive strength. This result was attributed to the particle structure of the organosilicon slag.
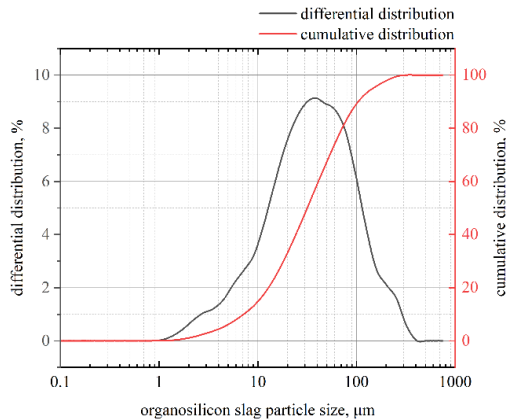

Fig. 4. The particle size distribution of the organosilicon slag

Fig. 4 depicted the particle size distribution curve for the organosilicon slag. The average particle size was determined to be 31.32μm with a dispersion of 3.34. A broad distribution was evidenced, wherein coarse particles constituted the majority. The undersize amounts of 30 mesh (550 μm), 40 mesh (380 μm), 50 mesh (270 μm) and 60 mesh (250 μm) were measured to be approximately 39.67%, 31.78%, 26.74% and 21.76% respectively of the total organosilicon slag amount.

Fig. 5 showed the self-ignition point test results for organosilicon slag. The black curve represented the organosilicon slag sample temperature, while the red curve showed the oven temperature. The oven was heated slowly at 0.5°C/min. Before ignition, the sample temperature matched the oven temperature closely. At 4 hours 46 minutes, the organosilicon slag ignited spontaneously, with the sample temperature rising far above the oven temperature. This phenomenon indicated that the self-ignition point for organosilicon slag was approximately 185°C. Since the typical drying temperature for exothermic insulating risers was around 180°C [7], the drying process for organosilicon slag risers needed to adjust appropriately.
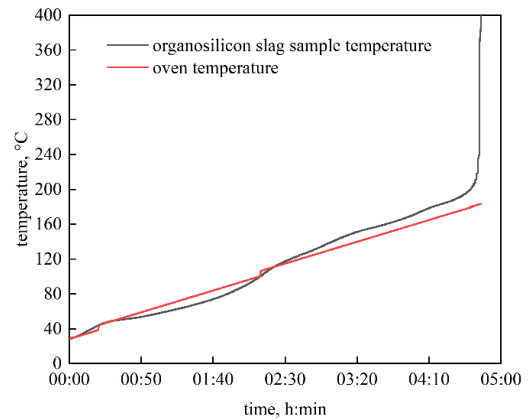

Fig. 5. The self-ignition point test curve for the organosilicon slag

4.2. Single-factor experiments on resol resin

4.2.1 The effect of resin viscosity on compressive strength
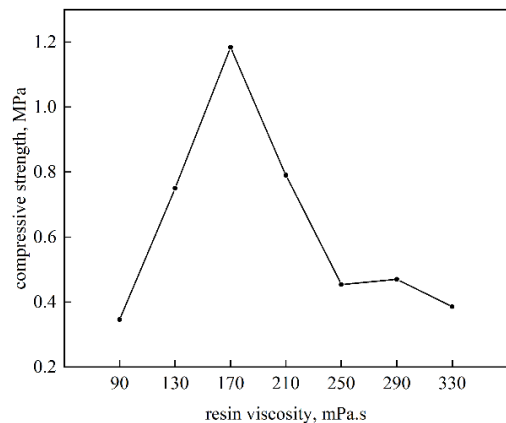

Fig. 6. The effect of resin viscosity on compressive strength

The binder viscosity amount was typically regarded as a variable impacting strength [10,11]. In the current study, ethanol was utilized as the diluent for the dilution of the resol resin at different ratios [12]. According to the viscosity of the binder used in the existing research of exothermic insulating risers, the resin viscosity after dilution would be 90, 130, 170, 210, 250, 290 and 330mPa.s, respectively. Risers were prepared with these resin binders in order to examine the effect of viscosity on compressive strength.

As shown in Fig. 6, the compressive strength exhibited an initial increasing trend followed by a decreasing trend with increasing resin viscosity. In the range of 90~350mPa.s, both too high or too low resin viscosity resulted in poor compressive strength of the specimens, reaching the peak value of 1.18MPa at 170mPa.s, indicating that the resin viscosity was more appropriate at this time.

4.2.2 Single-factor experiments on resin addition

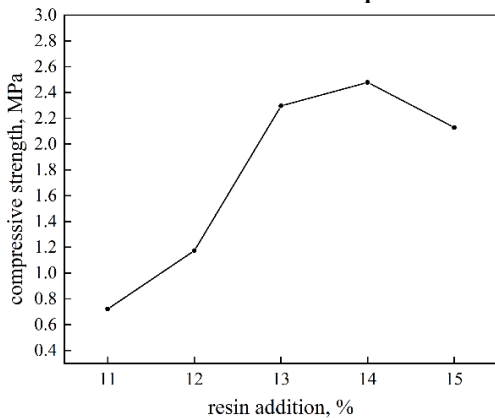#### 4.2.2.1. The effect of resin addition on compressive strength

Fig. 7. The effect of resin addition on compressive strength

Fig. 7 showed that the compressive strength of the samples increased overall as more resin was added. The strength increased more substantially between 12-13% addition. When the resin was 14% addition, compressive strength reached a maximum of 2.48 MPa. However, it subsequently slightly decreased to 2.1 MPa in 15% addition. Due to the loose and porous structure of the organosilicon slag, more resin was required for the riser to maintain its strength. That could explain the maximum strength at the 14% resin addition. When resin addition was 15%, although the resin-bonded bridge was hard to directly visible, the pores likely transferred from the particle contacts into the bridges themselves, resulting in porous bridge formation, which may have caused the slight decrease in compressive strength compared to the 14% addition [13].

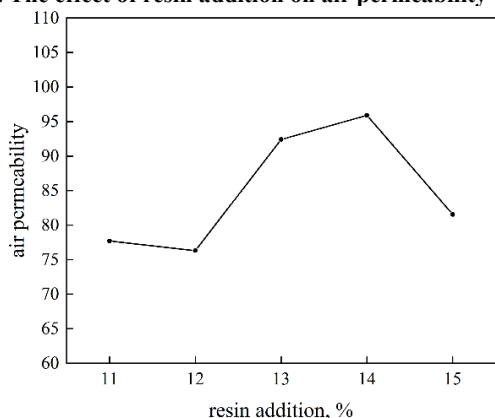#### 4.2.2.2. The effect of resin addition on air permeability

Fig. 8. The effect of resin addition on air permeability

Fig. 8 demonstrated the effect of resin addition on air permeability. Similar to the compressive strength, the air permeability had peaked at 95.9 with 14% resin addition. The air permeability between 11% and 12% resin addition had little change, probably because the resin primarily filled the surface pores of the organosilicon slag particles rather than forming resin-bonded bridges. Particle gaps did not get much broader. With resin addition increase, thicker resin films underwent greater shrinkage, widening particle gaps to improve air permeability. However, when the resin addition was 15%, excessive accumulation of resin between the particles could lead to blocking of the pore channels, consequently reducing air permeability [14]. Therefore, the optimal air permeability occurred at the balanced resin content, where shrinkage-induced pore widening was counteracted by pore blocking. In this experiment, both compressive strength and air permeability at 13% resin were close to those at 14%. In order to reduce the resin usage, the subsequent tests were carried out with the 13% resin addition.

4.3. Single-factor experiments on organosilicon slag

4.3.1. Single-factor experiments on slag addition

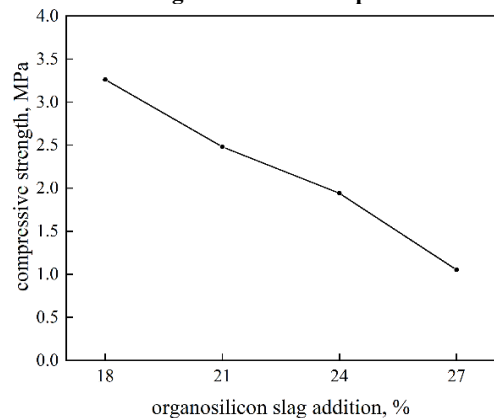#### 4.3.1.1. The effect of slag addition on compressive strength

Fig. 9. The effect of slag addition on compressive strength

As shown in Fig. 9, a nearly negative linear correlation was exhibited between the organosilicon slag addition and the compressive strength. The strength was found to be 3.26 MPa at 18% resin addition, which decreased to 1.05 MPa at 27% resin addition, representing a reduction of 67.8% in comparison to the 18% slag addition. This demonstrated the significant effect of the particle shape on strength. For an equal mass, spherical particles possess the smallest specific surface area. Greater deviation of the particle shape from spherical morphology led to increased surface area. With a fixed resin addition, the larger particle surface area gave rise to thinner resin films, consequently decreasing the bridge's cohesive strength [15]. A higher proportion of the slag increased the flocculent particle fraction in the riser material. During mixing riser materials with resin, the probability of the formation of thin resin films on the flocculent particles increased, leading to reduced compressive strength.

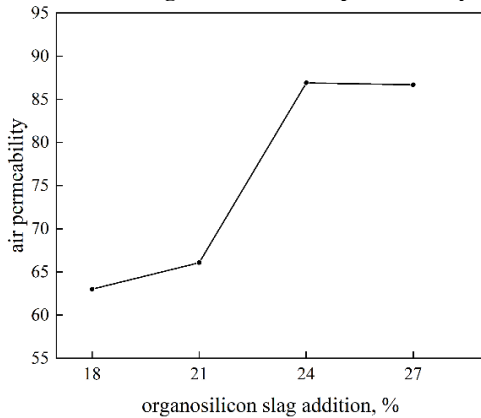#### 4.3.1.2. The effect of slag addition on air permeability

Fig. 10. The effect of slag addition on air permeability

As illustrated in the Fig. 10, in contrast to compressive strength, air permeability rapidly increased from 21% to 24% organosilicon slag addition, showing an overall positive correlation. Unlike spheres, irregular particles have smaller practical contact areas during packing, producing larger pores to improve air permeability. The data indicated air permeability reached optimal levels at 24% slag addition, with no further improvement at 27%. Despite the 3% increase in organosilicon slag proportion, the air permeability remained constant likely due to the limiting resin addition, which kept the pore channel number constant after mixing with riser materials. Higher slag additions could moderately enhance air permeability. However, considering compressive strength was prioritized, 18-21% organosilicon slag addition would be suitable for risers.

4.3.2. Single-factor experiments on slag particle size

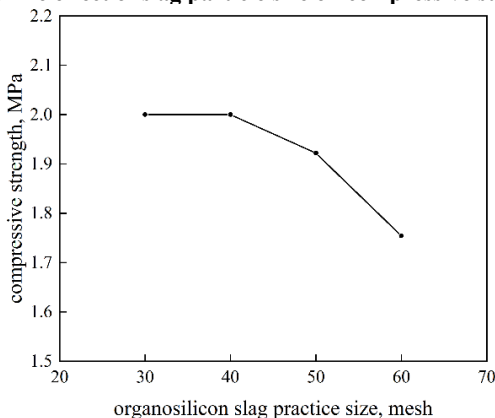#### 4.3.2.1. The effect of slag particle size on compressive strength

Fig. 11. The effect of slag particle size on compressive strength

As shown in Fig. 11, the compressive strength decreased gradually with increasing organosilicon slag particle size, reaching a maximum of 2MPa at both 30 mesh (550 μm) and 40 mesh (380 μm) undersize. Compared to other factors, particle size had a relatively small influence, causing only a 0.25MPa decline from 30 mesh (550 μm) to 60 mesh (250 μm) undersize. For spherical particles, the size itself did not affect strength theoretically. Smaller sizes had greater surface area, leading to thinner resin films but also more resin accumulation, increasing the bridge number – representing counteracting effects [16,17]. However, the organosilicon slag particles were irregular in morphology, worsening the shape at smaller sizes. This resulted in inter-particle bridging, poorer flow, and difficulty in compacting during preparation, consequently decreasing bridge formation. Additionally, the increase in surface area with reducing size was accompanied by an increase in surface pores. Therefore, the screening to smaller sizes led to a slight decrease in the compressive strength.

4.3.2.2. The effect of slag particle size on air permeability
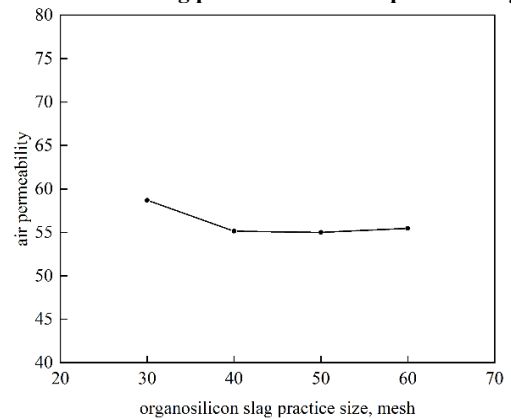

Fig. 12. The effect of slag particle size on air permeability

As shown in Fig. 12, insignificant changes were observed in the air permeability. A slight decrease from 58.7 to 55.13 was evidenced as the mesh size was reduced from 30 (550 μm) to 40 (380 μm). This could potentially result from the 30-40 mesh coarse particles comprising 20% of the 30 mesh (550 μm) undersize, thereby greatly influencing the pore channel size of the riser. The air permeability was found to remain stable at around 55 for the 40, 50, and 60 mesh sizes. Simply changing the organosilicon slag sieve mesh number had little effect on the air permeability.

4.4. Effects of the drying process on room temperature properties

In order to adjust the drying process [7], the changes in the dryness were recorded under different duration. Curve 1 in Fig. 13 depicted the profile for constant 180°C drying. Initially, from 0-25 min, a faster drying rate was evidenced, attaining an 80% dryness at 25 min owing to the shorter gel time and faster completion of resin gelation at higher temperatures. Beyond 25 min, the rate exhibited a gradual slowdown, approaching a constant weight at 50 min and completing curing by 60 min.
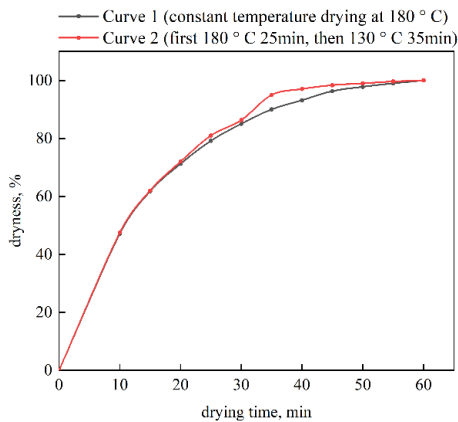
Fig. 13. Dryness curve of riser under different drying processes

Based on the observation of the drying degree change under constant 180°C, the drying process was adjusted to 25 minutes at 180°C initially, followed by decreasing the temperature to 130°C for 35 minutes. Curve 2 in Fig. 13 depicted the change in drying degree under this adjusted mode. In the first 25 minutes, the sample drying was analogous to that of constant temperature drying. Upon decreasing to 130°C after 25 minutes, the drying degree in the initial 5 minutes post temperature reduction remained similar to constant 180°C drying, likely due to residual heat within the sample itself. However, after those initial 5 minutes, the drying rate suddenly increased, exceeding 90% by 35 minutes. The sample attained a constant weight by 60 minutes. As resin shrinkage is lower at reduced temperatures, the riser dried with decreased temperature attained a constant weight sooner than that dried at a constant high temperature.
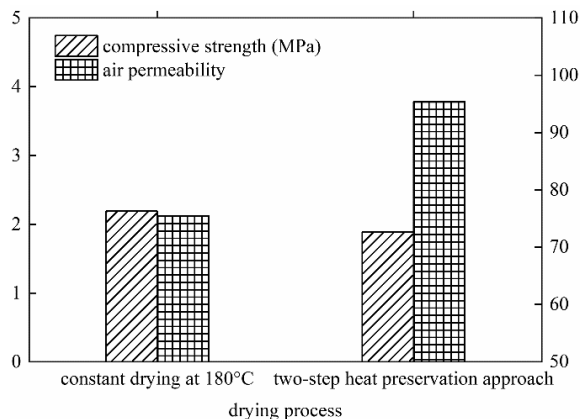

Fig. 14. Effect of drying process on compressive strength and air permeability

Effect of drying process on compressive strength and air permeability was shown in Fig. 14. Comparing these two drying processes, risers dried at the two-step heat preservation approach(180°C for 25 min and then 130°C for 35 min) exhibited slightly lower strength but superior air permeability in contrast to the constant temperature drying. The enhanced permeability could improve the heating performance of the risers. What's more, the subsequent experiments employing the two-step drying method did

not result in any self-ignition. Therefore, the optimal drying procedure was determined to be the two-step heat preservation approach with drying at 180°C for 25 minutes followed by 130°C for 35 minutes.

4.5. Orthogonal experiment

The optimization method from the literature optimized the following: A-resin viscosity, B-resin addition, C-organosilicon slag addition, D-organosilicon slag particle size [1]. The orthogonal tests and the extreme value analysis were shown in Table 4 and Table 5, respectively. For optimization of strength, the optimal combination was determined to be A3B3C2D1, while the optimal combination for permeability was A1B3C2D3. The range analysis revealed that resin addition exerted the most significant influence on both compressive strength and air permeability, followed by ethanol ratio, slag addition, and slag particle size.

Considering the priority of compressive strength, the optimized combination A3B3C3D1 was selected: 190mPa.s resin viscosity, 14% resin addition, 21% slag addition, and slag particle size of under 30 mesh (550 μm). The predicted values were 4.42 MPa strength and 64.1 air permeability. The tested preparation results were 4.21 MPa strength and 75.6 air permeability, which are close to predicted and meet existing standards.

Table 4.
Orthogonal test protocol and results

NO.	Factor				Index	
	A	B	C	D	Compressive strength	Air permeability
1	190	12	18	30	2.64	62.97
2	190	13	19.5	40	3.57	64.33
3	190	14	21	50	3.55	68
4	170	12	19.5	50	2.67	63.13
5	170	13	21	30	3.18	62.5
6	170	14	18	40	3.94	62.53
7	150	12	21	40	2.71	58.17
8	150	13	19.5	30	4.45	60.67
9	150	14	18	50	5.04	65.5

Table 5.
Means and extreme value of each factor for different indicators

Index	Level	A	B	C	D
Compressive strength	1	3.256	2.674	3.676	3.62
	2	3.263	3.734	3.761	3.41
	3	4.066	4.176	3.148	3.56
	R	0.810	1.501	0.613	0.216
Air permeability	1	65.10	61.42	62.06	63.66
	2	62.72	62.50	64.32	61.68
	3	61.44	65.34	62.89	63.93
	R	3.66	3.92	2.27	2.26

The comparative cost analysis was conducted between the optimized organosilicon slag made riser (OSR) formulated in this

study and the conventional aluminum powder made riser (APR) commercially available in the market. Table 6 showed the main raw material costs for both types of risers. It could be seen that the aluminum powder and resole resin have the highest costs among the riser materials. Under the condition that both risers could generate heat above 1500° C [1], the APR contained approximately 30% aluminum powder, 54.5% hollow floating beads, and 11% resole resin. In comparison, the OSR contained 14% aluminum powder, 21% organosilicon slag, 44.5% hollow floating beads, and 14% resole resin. Since both risers use the same amount of additives, the raw material cost for the APR was 9316.5 CNY per ton without considering the additives cost, while the raw material cost for the OSR was 6658.5 CNY per ton. This represented a 28.5% reduction in cost compared to the conventional aluminum powder made riser.

Table 6.
The main raw material costs for risers

Main raw material	Material unit price (CNY per ton)	Material proportion (%)		Material cost (CNY per ton)	
		APR	OSR	APR	OSR
aluminum powder	20300	30	14	6090	2842
organosilicon slag	3000	-	21	-	630
hollow floating beads	3700	54.5	44.5	2016.5	1646.5
resole resin	11000	11	14	1210	1540

Although the optimized riser met the strength requirements in pressure testing, further verification was needed to determine whether it could withstand the static pressure of molten iron without rupturing during actual casting. Risers cut from different feeding parts of a stainless steel casting were shown in Fig. 15. All the outer layer were organosilicon slag risers with the same formula of the optimized scheme, while the cavity was excess part formed by molten iron and slag during casting. The experiment focused on assessing the riser's compressive strength. Risers remained intact without any obvious cracks, indicating that excess molten iron did not crack them after concentrating in the riser. This demonstrated the riser had sufficient strength to withstand the static pressure of the molten iron. Beside that, visible differences could be found in riser appearance after casting: white silica powder were appeared on the outer side of Riser 1 and the entire Riser 2, demonstrating the different combustion degree of organosilicon slag. This likely due to varying molten iron temperatures at different feeding positions, ultimately affecting the combustion process of the riser. Overall, the intact risers confirmed that the riser prepared by the optimized scheme met the strength requirement.

Fig. 15. Risers cut from the casting

5. Conclusions

1) The organosilicon slag particles had a loose, porous, flocculent block structure. Due to its irregular shape, increasing organosilicon slag addition reduces compressive strength but improves permeability significantly. In contrast, risers decreased strength slightly with larger particle sizes but did not affect permeability. Therefore, the organosilicon slag of 18-21% addition and 30 mesh undersize would be more appropriate to prioritize compressive strength.
2) Both compressive strength and air permeability were influenced significantly by resol resin. However, either too high or too low resin viscosity or addition was unhelpful. With an appropriate viscosity of around 170 mPa.s and 13% addition, good compressive strength and air permeability can be achieved with minimal resin usage.
3) The drying process for risers added organosilicon slag was set to a two-step mode: first at 180 °C for 25 min, then at 130 °C for 35 min. Compared to drying at a 180 °C constant, It slightly reduced the compressive strength while improving air permeability and preventing self-ignition.
4) The optimal preparation scheme were 150 mPa.s resin viscosity, 14% resin addition, 21% slag addition, and slag particle size of less than 30 mesh (550 μm). Afterwards, the riser exhibited a compressive strength of 4.21 MPa and air permeability of 75.6, surpassing typical standards for exothermic insulating risers.

Acknowledgement

References

[1] Lu, J.J., Qian, J.B., Yang, L. & Wang, H.F. (2023). Preparation and performance optimization of organosilicon slag exothermic insulating riser. *Archives of Foundry Engineering*. 23(1),75-82. DOI: 10.24425/afe.2023.144283.

[2] Krajewski, P.K., Zovko-Brodarac, Z. & Krajewski, W.K. (2013). Heat exchange in the system mould - Riser - Ambient. Part I: Heat exchange coefficient from mould external surface. *Archives of Metallurgy and Materials*. 58(3), 833-835. DOI: 10.2478/amm-2013-0081.

[3] Vaskova, I., Conev, M. & Hrubovakova, M. (2017). The influence of using different types of risers or chills on shrinkage production for different wall thickness for material EN-GJS-400-18LT. *Archives of Foundry Engineering*. 17(2), 131–136. DOI: 10.1515/afe-2017-0064.

[4] Sowa, L., Skrzypczak, T. & Kwiatoń, P. (2022). Numerical evaluation of the impact of riser geometry on the shrinkage defects formation in the solidifying casting. *Archives of Metallurgy and Materials*. 67(1), 181-187. DOI: 10.24425/amm.2022.137487.

[5] Lu, J.J., He, W., Tan, S.M., Qian, J.B. & Lu, X. (2021). Chinese Patent NO. 202110970771.3. Beijing. China National Intellectual Property Administration.

[6] Wang, E.Z., He, J.Y., Shen, J. & Yan, F.Y. (1993). Permeability of washings for vacuum evapouration-pattern casting. *Special Casting & Nonferrous Alloys*. 6, 1-3. DOI:10.15980/j.tzzz.1993.06.001. (in Chinese).

[7] Yu, J., Wang, D.D., Mao, L., Li, C.Y., Lu, S.D., Xu, Q.B. & Wang, W.Q. (2008). Application of LYH-3 dextrin binder in exothermic and insulating riser. *Foundry Technology*. 7, 873-876. (in Chinese).

[8] Zhao, X., Wang, Z.X., Zhang, W.Q., et al. (2022). The Efficacy of magnetization in enhancing flocculation and sedimentation of clay particles. *Journal of Irrigation and Drainage*. 41(3), 114-124. DOI: 10.13522/j.cnki.ggps.2021300. (in Chinese).

[9] Cai, Y., Shi, B., Liu, Z.B., Tang, C.S. & Wang, B.J. (2005). Experimental study on effect of aggregate size on strength of filled soils. *Chinese Journal of Geotechnical Engineering*. 12, 1482-1486. (in Chinese).

[10] Kang, M., Wu, Y.L., Wang, W.Q. & Dai, X.Q. (1998). Effects of thermo - rheologic properties of thermo-plastic phenol resin on properties of resin-coated sand. *Modern Cast Iron*. 2, 11-13. (in Chinese).

[11] Dai, B.Y. (1996). Research on rheological property of phenol-formaldehyde resin for hot process. *China Foundry Machinery & Technology*. 5, 16-19. (in Chinese).

[12] Tang, L.L., Li, N.N. & Wu, P.X. (2008). *High performance phenolic resin and its application technology*. Beijing: Chemical Industry Press.

[13] Tong, L.L., Zhou, J.X., Yin, Y.J. & Li, Y.C. (2020). Effects of grain size and resin content on strength of furan resin sand. *Special Casting & Nonferrous Alloys*. 40(2), 139-142. DOI:10.15980/j.tzzz.2020.02.005. (in Chinese).

[14] Wang, W., Li, X.H., Gao, P.H., Zeng, S.C., Chen, B.Y., Yang, Z., Guo, Y.C. & Li, J.P. (2021). Study on optimization of gas evolution in resin sand moulds. *Hot Working Technology*. 50(15), 48-50. DOI:10.14158/j.cnki.1001-3814.20192900. (in Chinese).

[15] Li, C.S. (2012). Influence of properties and state of raw sand on properties of self-setting resin sand. *Modern Cast Iron*. 32(5), 63-68. (in Chinese).

[16] Zhu, Y.L. & Cai, Z.S. (1996). Analysis of the influence of original sand particle size on the strength of resin bonded sand. *Foundry*. 12, 37-38. (in Chinese).

[17] You, M. & Zheng, X.L. (1999). Theoretical analysis of the influence of original sand particle size on the strength of resin bonded sand. *Foundry*. 2, 42-44. (in Chinese).